On the Performance Evaluation of Two Novel Fractional Frequency Reuse Approaches for OFDMA Multi-User Multi-Cellular Networks

Maria A. Seimeni (1), Georgios I. Tsivgoulis (1), Panagiotis K. Gkonis (1), Dimitra I. Kaklamani (1),
Iakovos S. Venieris (1) and Christos A. Papavassiliou (2)

(1) National Technical University of Athens, School of Electrical and Computer
Engineering, 9 Heroon Polytechneioy str, Zografou, Athens, Greece
(Email: mseimeni@icbnet.ntua.gr, gtsivgou@icbnet.ece.ntua.gr, pgkonis@esd.ntua.gr, dkaklam@mail.ntua.gr,
venieris@cs.ntua.gr)

(2) Electrical and Electronic Engineering, Imperial College, South Kensington Campus,
London SW7 2AZ, England
(Email: c.papavas@imperial.ac.uk)

***Abstract*—The paper studies two resource allocation strategies (*GRID, anti-EMI*) for Multi-User Orthogonal Frequency Division Multiple Access (MU OFDMA) systems. These strategies are evaluated after being compared with the *Round Robin* and the *Fractional Frequency Reuse* (*FFR*) strategy in terms of mean throughput and mean dissipated power for 1, 2 and 5 allocated subcarrier frequencies per mobile terminal (MT) and algorithmic complexity. All investigated strategies assign resources without Channel State Information (no CSI), while both *GRID* and *anti-EMI* inherently combat Co-Channel Interference (CCI); hence they enhance mean throughput. Simulations indicate that *GRID* outperforms *Round Robin* and *FFR* in all scenarios into consideration and competes the *anti-EMI* strategy in various network orientations. The latter is justified especially for highly populated scenarios (i.e. 50% probability failure and 2 subcarriers per MT). As for the *FFR* strategy, simulations verify that the spectral efficiency is not the optimum in irregular-shaped cell networks, which has been verified in studies on regular-shaped cell networks as well. Finally, the platform can inherently spare around the 70% of the maximum available power.**

***Index Terms*—OFDMA, Resource Allocation Management, FFR, Inter-Cell Interference Coordination.**

I. INTRODUCTION

Like all infrastructure-based wireless networks, a multi-cellular network is a cluster of coordinated base stations (BS, fixed access points) which ensures access for the mobile terminals to a backbone wired network with a single-hop routing. Even though from the financial and practical perspective it is not easily deployed, it is preferred over an ad-hoc network because it can enhance spectral efficiency thanks to frequency reuse, supports higher data rates, while also decreases delay and losses. However, the tendency of the MTs to further increase in number [1], the fast ubiquity of the new technologies along with the digital nomadic lifestyle resulted in a rather scarce spectrum and amplified the need for enhanced spectral efficiency and throughput, judicious exploitation of the available resources and interference mitigation.

To deal with the aforementioned issues, this study focuses primarily on multiple access schemes and anti-jamming resources management (PHY, MAC) that are both based on the Orthogonal Frequency Division Multiplexing (OFDM) scheme [2]. This scheme has been widely taken into consideration especially for the last two technology generations, that is to say 3G and 4G, as in the case of IEEE standard-based technologies: WiMAX (802.16) [3], Bluetooth (802.15.1) [4], WiFi (802.11) [5] and WRAN (802.22) [6], and has been scheduled to be included in the next to come technology era (i.e. 5G).

Inherently, OFDM enhances spectral efficiency due to the orthogonality between the adjacent subcarriers and can combat fading (owing to multipath and shadowing) by dividing a fast fading channel into flat fading narrowband sub-channels. If the aforementioned characteristics are combined with the multi-user diversity in frequency domain (i.e. in MU-OFDMA access scheme: different terminals experience a different channel quality and, therefore, a terminal is assigned a good-quality channel) [7], then the throughput challenge may be addressed. The effectiveness of the multiple access scheme has proved to be high, which is also witnessed by the recent scientific efforts to implement it on the Carrier Sense Multiple Access/ Carrier Aggregation (CSMA/CA) of LAN topologies [8]-[14]. OFDMA [15] cannot be easily implemented even though it is simple in principle, because radio resources are scarce to find, interference is still present (i.e. Co-Channel Interference, CCI), the MTs have different Quality of Service (QoS) requirements, etc.. If efficient resource allocation strategies are adopted, then these challenges can be addressed through trade-offs.

To this end, Inter-Cell Interference Coordination (ICIC) techniques deal with interference issues or in other words can lead to the mitigation of the SINR degradation. Usually, these techniques can be either Static or Cooperative and can be grouped into Interference Mitigation Techniques (IMT) and Interference Avoidance Techniques (IAT). Yet, it is anticipated that in the end they will be combined in the fast-emerging technologies in order to jointly provide the best out of them.

Several scientific efforts have been published on this topic until now, including FFR-based strategies due to their low complexity and ease of implementation. Efforts in [16]-[19] divide the cell in regions (inner, edge) in order to optimize the system. In detail, the technique described in [16] groups users and subcarriers to each region and increases data rates and mitigates ICI, [17] improves system's capacity and data rates, [18] improves the receivers' performance without CSI, while the proposed algorithm in [19] applies optimal frequency allocation to maximize the total cell throughput. The algorithm introduced in [20] divides the edge-region of each cell into three sectors and is based on maximizing the average sector data rate subject to a minimum cell-edge data rate. Finally, in [21], authors attempt to improve the system capacity with an exhaustive manner through an adaptive Soft Frequency Reuse (SFR) algorithm.

Unlike the above papers which all refer to regular cellular layouts, studies in [22]-[33] focus on Radio Resource Management (RRM) for irregular cell-networks as in our case. In detail, in [22] Gonzalez *et al.* compare Reuse-1 model, Reuse-3 model, SFR and full isolation FFR models in irregular cellular configurations and draw their attention to the trade-off between efficiency and fairness. However, the related documentation is not openly available as in the case of the documentation of the European Momentum project [25], where a realistic radio propagation setting is included and then used in irregular cell networks [24]. In [26], the efforts extend the studies of [27] by proposing an algorithm that optimizes the *FFR* scheme for realistic (irregular cell layout) networks and is based on a multi-objective approach [28]. To this end, good QoS, spectral efficiency maximization and reduction of the power dissipation are attempted to be jointly addressed at the cost of the computational complexity. Although the complexity of the proposed algorithm is governed by the NSGA-II [29], i.e. $O(MN^2)$, where N and M are the population size and the number of objectives respectively, the computational cost depends on the scale of the network, the resolution of the pixels, the number of cells and the size of the channel gain. The studies in [30] and [31], the studies propose a generalizing *FFR* (GFFR) scheme which degrades spectral efficiency, estimates the appropriate number of sub-bands in an exhaustive iterative manner, whereas it is applicable for realistic network scenarios. More precisely, according to the GFFR, the sub-band assigned to the inner sub-region of the cell is the same for all cells and the cell-edge sub-band is partitioned for all cells into the same set of multiple sub-bands. The set of multiple sub-bands is, then, further divided into subsets of different lengths. The sub-bands which constitute a subset are assigned the same power level, yet different from the power levels of the other subsets. Finally, the subset allocation is cell-specific. In [32], the knowledge of the terminals' position (which can be available for the smart-phones) and their available resources (power, subcarriers) dynamically self-organize the proposed *FFR* scheme. According to the algorithm, based on the terminals distribution and the presence of hotspots in each sector of a cell, the center of gravity for each cell is calculated, the system is dynamically modelled and autonomously adapts both the inner and the cell-edge sub-regions and thus the resource allocation to the terminals. Then, the system performance is evaluated and if the average SINR per sector is lower than a predefined value the system is re-modelled accordingly.

Finally, due to the fact that the performance of a wireless cellular system is directly related to the BSs position [33] (the next technology generation systems mandate that the BSs are randomly deployed), in [34]-[37] the spatial configuration of the base stations is also addressed. The majority of the existing studies implement ideal, over-simplified, inaccurate and non-realistic models until recently such as the single cell model (which does not consider Inter-Cell Interference), the Wyner model (which considers equal Inter-Cell Interference) and the Hexagonal Grid model (which considers normally distributed BSs and mandates exhaustive simulations to evaluate the performance of complex systems).

However, all the above studies and all research on *FFR* schemes in general are focused on the standard hexagonal shaped cellular configurations. The hexagonal shape is indeed convenient for theoretical research and simulations, but it appears rather poor in realistic network scenarios where real-time optimization is required on a constant basis to improve the network's performance. As a matter of fact, in real scenarios the coverage area coincides with the amoeba-like shape rather than with the traditional shape (hexagon, rectangle, triangle, etc.). This along with the frequency planning, which is required in advance and is difficult to implement especially in the Heterogeneous Networks where macro/pico/femto-cells are ad-hoc allocated, make the *FFR* schemes apparently poor and difficult to implement in real life networks [22]-[24].

Motivated by the FFR mindset, this paper studies two resource allocation strategies along with the traditional *FFR* and the *Round Robin* algorithms for amoeba-like multicellular systems. The first introduced algorithm, namely *GRID*:

- dynamically plans and spatially isolates the radio resources that are available to each cell by partitioning them in disjoint subsets and, hence, mitigates CCI;
- enhances spectral efficiency (with respect to the traditional *FFR* scheme);
- boosts system capacity;
- does not load the system with additional overhead (i.e. no CSI);
- adds less computational overhead than the traditional *FFR* to the system.

The second algorithm (anti-EMI algorithm) is an MT-centric *FFR* scheme and combats electromagnetic interference (EMI) owning to co-channel transmissions. Each time a new terminal gains access to the network, the available subcarriers of the serving BS are classified into two groups: those reused by *Jammers* and those reused by *non-Jammers*. The *non-Jammers*' subcarriers are taken into consideration and a wish list is created. This list is actually the result of the cooperation established between the neighboring BSs and the last accepted MT and contains a certain subset of *non-Jammers*' subcarriers. Finally, the wish list is communicated between the cells through the X2 interface [38]-[39] in order to prepare them for downlink (DL) transmission. Therefore, the second strategy:

- dynamically protects each terminal against CCI by allocating the subcarriers which are not reused by *Jammers* and hence, inherently mitigates CCI;
- enhances spectral efficiency;
- enhances system capacity;
- does not load the system with additional overhead (CSI);
- adds low computational overhead to the system.

The procedure of power allocation per subcarrier frequency per MT is uncoupled from the subcarriers allocation procedure and, therefore, is handled by the platform itself.

The rest of this paper is structured as follows: The network architecture and the simulation platform are described in Sections II and III respectively. In Section IV, we present the proposed resource allocation strategies, while in Section V the algorithmic complexity is discussed. Finally, simulations and conclusions are provided in Sections VI and VII respectively.

II. NETWORK ARCHITECTURE

This study considers DL transmission scenarios of a multicellular network at 2.5 GHz carrier frequency. The base stations are regularly located on the spatial area and are equipped with a three-beam directional antenna with radiation pattern (1) as specified by [40] (see Fig. 1):

$$f(\varphi) = BG_b - \min\left[12\left(\frac{\varphi-\varphi_k}{\varphi_{3dB}}\right)^2, A_m\right] \qquad (1)$$

for φ_k-$60^o \le \varphi \le \varphi_k$+$60^o$. In (1), φ_k is the antenna boresight at sector k, BG_b is the broadside antenna gain, φ_{3dB} is the 3-dB beamwidth of the antenna pattern, and A_m is the front-to-back ratio gain. All simulation parameters of the network into consideration are summarized in Table I.

In our case, due to the fact that a MT pairs with the BS with the lowest path losses (best signal quality), no matter what the distance between them (near, far), in the end the served MTs conceptually form cells of arbitrary shapes; hence cell boundaries coincide with the amoeba shape of the coverage area (see Fig. 2) and not with traditional shapes.

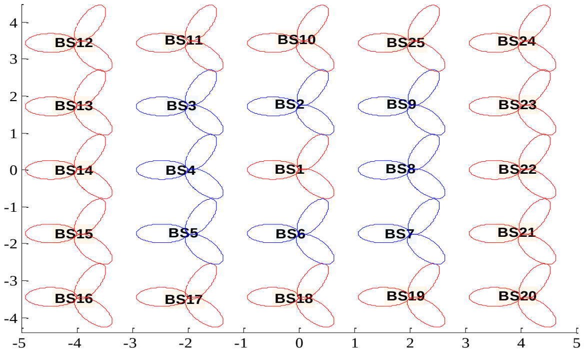

Fig. 1. The 3-beam antenna boresights for a 2-tiers multi-cellular network (top view, horizontal and vertical axis are expressed in Km).

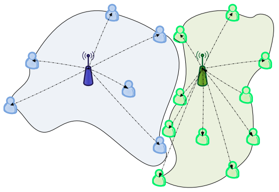

Fig. 2. Two amoeba shape cells (i.e. **blue cell**, **green cell**). The MTs of each BS form a coverage area of arbitrary shape. ***The space between the coverage areas is negligible.***

TABLE I. SIMULATION PARAMETERS

Parameter	Value
Tiers	1, 2
Vertical/ Horizontal Distance of BSs	1.73 *km* / 2 *km*
Cell geometry	Arbitrary shape / Sectorized
BS /MT height	30m/1.5 m
Propagation	COST 231 Hata model [41]
Standard deviation for shadow fading	8 dB
Azimuth dispersion	Laplacian distribution, azimuth spread 5°
Radiation pattern of the antenna array [40]	Broadside gain = 14 dBi $\varphi_k \in \{60^o, 180^o, 300^o\}$ 3-dB beamwidth = 70° Front-to-back ratio = 20 dB
Subcarrier frequencies per MT	1, 2, 5
Failure Probability (*PF*)	30%, 50%
Number of Monte Carlo (MC) runs	10^3
Thermal noise level at MTs (I_{noise})	-104 dBm
Maximum power per eNB /MT	43/30 dBm
SINR	9.6 dB [42] (QPSK modulation)
Carrier frequency	2.5 GHz
Total subcarriers per sector, *C*	128
Total sub-blocks per block, *G*	4, 9, 16, 25, 36
Jammers Range, *JR*	1*Km*, 1.5*Km*
Total Bandwidth/ Subcarrier Bandwidth	10 MHz/ 78.125KHz

III. SIMULATION PLATFORM

The platform executes a sufficient number of Monte Carlo runs (MC) to simulate a realistic traffic scenario. Each iteration comprises four steps, Fig. 3. The platform is semi-static, because during a MC run the MTs do not change their position. It is also noted that a MT is defined by a set of variables such as its geographical location, total losses due to multipath fading, set of subcarrier frequencies and power.

For a MC run, MTs enter the system sequentially (randomly located on the spatial area) following a Gaussian distribution i.e. *CN(0,1)* and do not change their location till the snapshot is over, ***Step 1*** (*Access attempt*). Since the device of each n^{th} MT ($1 \le n \le N$) operates in a rich EM scattering environment, path losses (shadowing is included as a Gaussian distribution, *CN(0,1)*) have to be taken into consideration. As such, n^{th} MT will request service from the b^{th} BS ($1 \le b \le B$) with the lowest pathloss, (***Step 2***: *Service request*). If the lowest pathloss exceeds a predefined value, the terminal is rejected, otherwise the total losses are estimated. In ***Step 3*** (*Waveform assignment*), the b^{th} BS assigns without any CSI a U_n set of subcarrier frequencies according to the algorithms described in the following section. Since our approach is multi-objective (dynamic power estimation, subcarriers allocation, fairness maintenance among terminals, reduced algorithmic complexity, etc.), a fixed number of subcarriers per terminal is considered (i.e. $S_n = |U_n|$). Then, in ***Step 4*** (*Dynamic transmission power assignment-power control*), the subcarrier frequencies of the n^{th} terminal are assigned a power level $p_{n,s}$ (2):

$$p_{n,s} = \left(\frac{E_b}{N_o}\right)_{n,s} \left(\sum_{k=1,k\neq i}^{K} P_{k,s} \frac{TL_{n,i}}{TL_{n,k}} + \mathrm{I}_{\mathrm{noise}} TL_{n,i} \right) \quad (2)$$

where $p_{n,s}$ is the transmission power for the n^{th} MTs and s^{th} subcarrier ($1 \le s \le S$), K denotes the number of effective sectors, i is the serving sector of the n^{th} MT and $P_{k,s}$ is the total transmission power of the k^{th} sector that has been allocated to the s^{th} subcarrier. Moreover, $\mathrm{I}_{\mathrm{noise}}$ is the total received thermal noise from the n^{th} MT and $TL_{n,i}$ and $TL_{n,k}$ are the total losses of the n^{th} MT for the i^{th} and k^{th} sectors respectively. E_b is the power of the received signal and N_o is the noise power.

If $p_{n,s}$ power level exceeds 1 Watt (3a,b), the terminal is rejected, its subcarriers are disengaged and the process repeats for the next candidate terminal. It is also noted that each subcarrier frequency is assigned to no more than one terminal (3c).

$$0 < p_{n,s} \le 1 \quad (3a)$$

$$0 < \sum_{s=1, s\in S_n} p_{n,s} \le 1 \quad (3b)$$

$$S_n \cap S_i = \varnothing, \quad \forall n,m \in N, \quad n \neq m \quad (3c)$$

S_n indicates the set of subcarrier frequencies assigned to the n^{th} MT. The MC simulation stops once probability failure (*PF*, number of rejected terminals per total number of access requests) exceeds a predefined value.

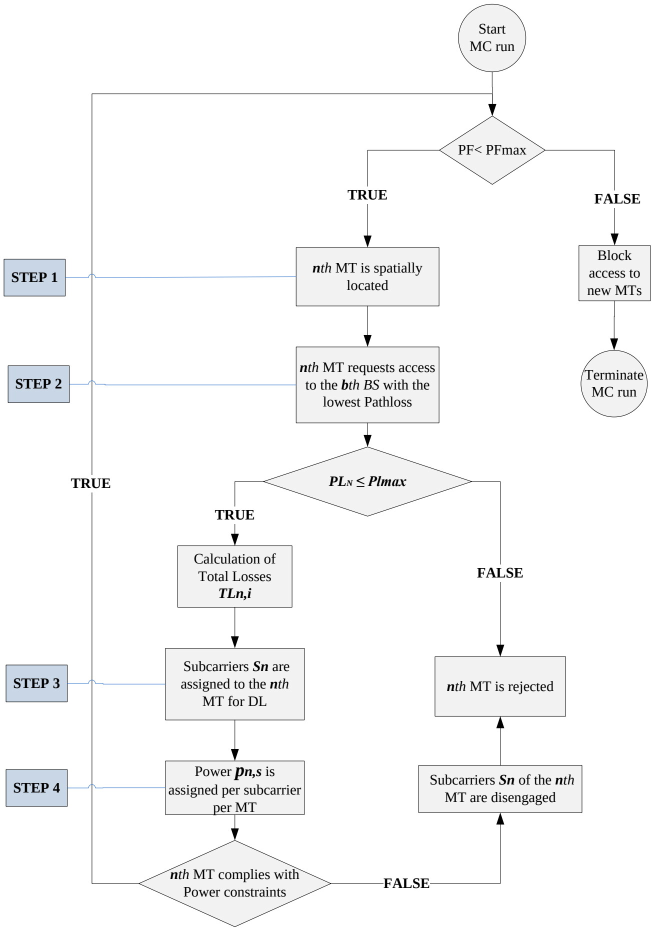
Start MC run
PF< PFmax
TRUE
FALSE
Block access to new MTs
Terminate MC run
STEP 1
nth MT is spatially located
STEP 2
nth MT requests access to the bth BS with the lowest Pathloss
TRUE
PLN ≤ Plmax
TRUE
FALSE
Calculation of Total Losses TLn,i
STEP 3
Subcarriers Sn are assigned to the nth MT for DL
nth MT is rejected
STEP 4
Power pn,s is assigned per subcarrier per MT
Subcarriers Sn of the nth MT are disengaged
nth MT complies with Power constraints
FALSE

Fig. 3. Monte Carlo simulation flow.

IV. RESOURCE ALLOCATION ALGORITHMS

This section presents the proposed strategies (*GRID*, *anti-EMI*) along with the classical *Round Robin* radio resource exploitation and the enhanced version of the *FFR* strategy, which lacks intelligence. All the algorithms (Step 3, Fig. 3) manage resources without CSI, while both the *anti-EMI* and *GRID* algorithms inherently combat CCI at the cost of algorithmic complexity.

A. Round Robin Algorithm

As the name implies, the b^{th} BS assigns the first S_n available subcarriers to the n^{th} accepted terminal at the k^{th} sector in a round robin manner. The algorithm lacks intelligence as it does not consider interference.

$$\begin{aligned} U_n &\leftarrow C_b\left(1:S_n\right) \\ C_b &\leftarrow C_b \setminus U_n \end{aligned} \quad (4)$$

where C_b indicates the set of available subcarriers of the b^{th} BS.

B. FFR Algorithm

Like traditional *FFR* strategy, the inner sub-regions are assigned the same subset (i.e. 1) of subcarriers, but at different power levels (p1, p3, p5, p8, etc.). The remaining subset of subcarriers is further partitioned (i.e. 2, 3, 4, 5). More precisely, sub-band 1 includes half of the available subcarriers per sector (i.e. 1-64), while the rest sub-carriers are partitioned orthogonally in disjoint subsets of equal length (i.e. 65-80, 81-96, 97-112, 113-128) and different power profile, which in turn is also dictated by the platform itself, Fig. 4.

Assuming that the three sectors are denoted by i.e. k_1, k_2, k_3, the five sub-bands are denoted by SB_1, SB_2, SB_3, SB_4, SB_5, the power levels are denoted by p_1, p_2, p_3, p_4, etc. and the inner sub-region (cell-edge sub-region) is denoted by r_1 (r_2), then the *FFR* scheme can be explained by the following set of equations.

$$\begin{aligned} &k_1 = k_2 = k_3 \\ &k_{1,\text{Cell 1}} = \{SB_1(p_1,r_1), SB_2(p_2,r_2)\} \\ &k_{1,\text{Cell 2}} = \{SB_1(p_3,r_1), SB_3(p_4,r_2)\} \\ &k_{1,\text{Cell 3}} = \{SB_1(p_5,r_1), SB_4(p_6,r_2)\} \\ &k_{1,\text{Cell 4}} = \{SB_1(p_8,r_1), SB_5(p_7,r_2)\} \end{aligned} \tag{5}$$

Once the MT is spatially located, then it is randomly assigned subcarriers from the sub-band which corresponds to its cell-type and sub-region by using the *randsample(i,D)* function. The function returns randomly *i* elements from *D* set.

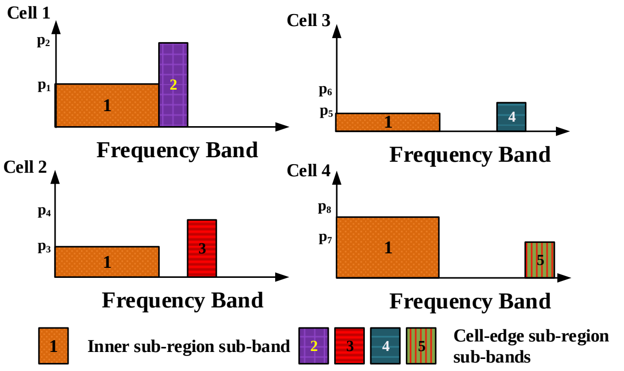

Fig. 4. Four cell types of the slightly new version of the traditional FFR strategy.

C. *Anti-EMI Algorithm*

This algorithm is MT-centric, as it dynamically protects each terminal against CCI by avoiding the allocation of the subcarriers which are reused by the MTs of neighboring BSs within a certain range (in other words *Jammers*), hence, CCI is mitigated. In detail, each time a new terminal gains access to the network, the strategy virtually partitions the area around each new candidate n^{th} MT into two sub-regions. The partitioning is done according to a predefined distance (*Jammers Range*, *JR*) and as a result the MTs of the neighboring BSs are classified into *Jammers* and *non-Jammers*. The available subcarriers of the serving BS are also classified into two groups: those reused by *Jammers* and those reused by *non-Jammers*. The *non-Jammers'* subcarriers are taken into consideration to create the *wish list*. This list is actually the result of the cooperation established between the neighboring BSs and the last accepted MT and contains a certain subset of *non-Jammers*' subcarriers. Finally, the *wish list* is communicated between the cells through X2 interface [39] in order to prepare them for downlink (DL) transmission.

If U_n is a subset of C_b assigned to the n^{th} MT at the k^{th} sector, then the n^{th} MT must not reuse subcarriers which are "virtually" engaged by the *Jammers*. However, if all the available subcarriers of the b^{th} BS are "engaged" by *Jammers*, the n^{th} MT has to reserve subcarriers randomly. The pseudocode of the *anti-EMI* algorithm is given by:

```
if    $C_b \cap C^*_{CJ} = \varnothing$
          $C_b \leftarrow C_b$                        $\rightarrow$  $U_n \leftarrow randsample(S_n, C_b)$      (6)
else                                               $C_b \leftarrow C_b \setminus U_n$
          $C_b \leftarrow C_b \cap C^*_{CJ}$
end
```

where C^*_{CJ} is the set of subcarriers which are not assigned to the *Jammers*.

A relevant example is given in Fig. 5. Supposing that the last accepted terminal is the red one, which is served by the blue BS, then before engaging any radio resource, a *wish list* has to be created. The algorithm mandates that the list must not include the subcarriers which are engaged by the green terminals (#1, #2, #3), which are served by the green BS and are within the *JR*. As a result, the *Jammers* of this example are all those green terminals (#3) engulfed by the arc (red bold line).

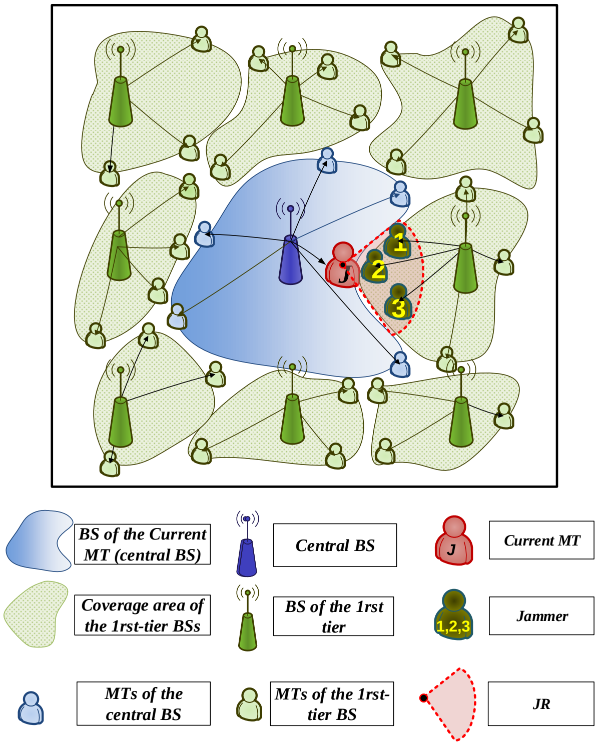

Fig. 5. The red MT must not reuse the subcarrier frequencies which are already assigned to the *Jammers*. *Jammers* are the green MTs which are enclosed in the red semi-cycle (terminals within *JR* distance from the red MT). ***The space between the coverage areas is negligible.***

D. *GRID Algorithm*

The GRID algorithm dynamically plans and spatially isolates the radio resources that are available to each cell by partitioning them in disjoint subsets as shown in Fig. 6. In detail, the mechanism conceptually grids the spatial area into disjoint equal blocks (blue rectangles), one for each BS, while each block is further partitioned in G ($1 \le g \le G$, $\sqrt{G} \in$

ℕ) disjoint equal sub-blocks (red rectangles). Prior to each MC simulation, the algorithm "virtually" pre-allocates to each sub-block g_b of the b^{th} base station a subset $f_{b,g}$ ($1 \le f \le F$, $length(f) = floor(C,G)$) of subcarrier frequencies, (Table II, Line 6). It is noted that each subcarrier subset appears only once in each block, all subsets have equal lengths and are disjoint; hence a subcarrier belongs to only one subset. Moreover, the sub-blocks are assigned dynamically different power levels, Fig. 7. In case the remainder equals zero, $rem(C,G) \neq 0$, then the last $rem(C,G)$ subcarrier frequencies are used in case that all frequency subsets are empty (Table III, Lines 6-7).

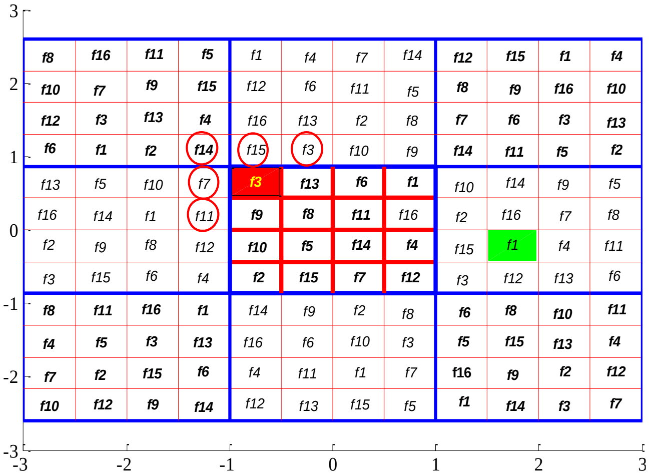

f8	f16	f11	f5	f1	f4	f7	f14	f12	f15	f1	f4
f10	f7	f9	f15	f12	f6	f11	f5	f8	f9	f16	f10
f12	f3	f13	f4	f16	f13	f2	f8	f7	f6	f3	f13
f6	f1	f2	f14	f15	f3	f10	f9	f14	f11	f5	f2
f13	f5	f10	f7	f3	f13	f6	f1	f10	f14	f9	f5
f16	f14	f1	f11	f9	f8	f11	f16	f2	f16	f7	f8
f2	f9	f8	f12	f10	f5	f14	f4	f15	f1	f4	f11
f3	f15	f6	f4	f2	f15	f7	f12	f3	f12	f13	f6
f8	f11	f16	f1	f14	f9	f2	f8	f6	f8	f10	f11
f4	f5	f3	f13	f16	f6	f10	f3	f5	f15	f13	f4
f7	f2	f15	f6	f4	f11	f1	f7	f16	f9	f2	f12
f10	f12	f9	f14	f12	f13	f15	f5	f1	f14	f3	f7

Fig. 6. Blocks (blue rectangles) and sub-blocks (red rectangles) for 1 tier of base stations (G =16). Subcarrier frequency subsets f per sub-block per block for 1 tier of base stations, edge sub-block (red) and inner sub-block (light green). (top view, horizontal and vertical axis are expressed in Km)

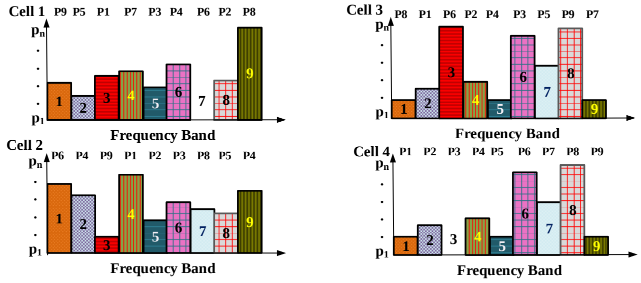

Fig. 7. The power which is consumed in the sub-blocks of four different cells. In example, sub-block 4 of Cell 1 consumes P7 Watts, sub-block 9 of Cell 2 consumes P4 Watts, sub-block 1 of Cell 3 consumes P8 Watts, sub-block 6 of Cell 4 consumes P6 Watts and so forth. Moreover, sub-block 7 of Cell 1 and sub-block 3 of Cell 4 do not consume power simply because there is no MT therein. Therefore, P6=0 Watts and P3=0 Watts respectively.

In Tables II-III, |Y| denotes the quantity of sub-blocks, subcarrier subsets, etc., *floor(X/Y)* rounds the quotient to the nearest lower integer, while *rem(C,G)* indicates the remainder after the division of *C* by *G*.

In particular, after function ***grid()*** has been executed, subcarriers S_n must be assigned. Supposing that *b*' is the base station where the terminal geographically belongs and *b* is the base station which serves it, there are two cases that have to be examined (Table III):

- **Case 1** - If *b*' = *b* (Line 1); hence the terminal is served by b^{th} and spatially belongs to the b^{th} BS, then its geographical sub-block is $g_{b,n}$ (Line 2).
- **Case** 2 - If $b' \neq b$; hence the terminal is served by the b^{th} BS but does not spatially belongs to the same BS, then the MT is hypothetically located to a geographical sub-block of the *b* BS. This sub-block is randomly selected as indicates Line 4.

TABLE II. FUNCTION ***grid()***

```
(1) $length(f) = floor(C/G), \forall f \in F$
(2)   for   $1 \le b \le B$
(3)       for   $1 \le j \le |F|$
(4)           $g_b \leftarrow randsample(1, G_b)$
(5)           $G_b \leftarrow G_b \setminus g_b$
(6)           $f_{g_{b,n}} \leftarrow [(j-1)*length(f)+1]:[j*length(f)]$
(7)       end
(8)   end
```

TABLE III. ***GRID()*** ALGORITHM

```
(01) if   $b == b'$
(02)     $g_{b,n} \leftarrow g_b$
(03) else
(04)     $g_{b,n} \leftarrow randsample(1, G_b)$
(05) end        $(if\_in\_line\_1)$
(06) if   $f_{g_{b,n}} = \varnothing$,   for   $\forall g \in G_b$
(07)     $U_n \leftarrow randsample(S_n, (|C_b| - rem(|C_b|, G)+1):|C_b|)$
(08) else
(09)     if   $f_{g_{b,n}} \neq \varnothing$
(10)         $U_n \leftarrow randsample(S_n, f_{g_{b,n}})$
(11)     else
(12)         if   $g_{b,n}$   edge   sub-block
(13)             $g_{b,n} \leftarrow g_{b,l}$
(14)         elseif   $g_{b,n}$   inner   sub-block
(15)             $g_{b,n} \leftarrow randsample(1, G_b)$
(16)         end        $(if\_in\_line\_14)$
(17)         $U_n \leftarrow randsample(S_n, f_{g_{b,n}})$
(18)     end        $(if\_in\_line\_10)$
(19) end        $(if\_in\_line\_6)$
(20) $f_{g_{b,n}} \leftarrow f_{g_{b,n}} \setminus U_n$
(21) $C_b \leftarrow C_b \setminus U_n$
```

Once the sub-block of the n^{th} MT is decided, then subcarriers S_n must be extracted from the subset $f_{g_{b,n}}$, which corresponds to the its sub-block $g_{b,n}$ (Table III, Lines 09-10). If $f_{g_{b,n}}$ is empty, then the terminal has to borrow subcarriers from other subcarrier subsets of b^{th} base station. In case $g_{b,n}$ is an *edge sub-block* (Table III, Lines 12-13), then attention must be paid to wisely select the new subcarrier subset. For example, an *edge sub-block* is the sub-block of the BS1 filled with red, Fig. 6. This sub-block has been pre-assigned (Table II) the subcarrier subset *f3*. To avoid interference issues, a MT located at this sub-block must not reserve radio resources from subcarrier subsets which are also assigned to *edge sub-blocks* of neighboring BSs (here g_b^*: *Jamming Edge Sub-Blocks, J*). In this example, it is straightforward that the MT must not reserve subcarriers from {*f7, f11, f13, f14, f15*}. If, however the terminal belongs to an *inner sub-block* (Table III, Lines 14-15), there are no constraints in reserving subcarriers and the candidate sub-block is randomly selected. An *inner sub-block* is considered to be the one of the BS8 filled with light green. Finally, it is noted that each sub-block of each cell is dynamically assigned a power level.

V. ALGORITHMIC COMPLEXITY

Likewise [26], the complexity in our case depends exclusively on the number of cells, the number of the allocated subcarriers per MT and number of concentric sub-regions/*Jammers*/*sub-blocks per cell* (traditional *FFR*/ *anti-EMI*/ *GRID* respectively).

For the *Round Robin*, to assign S_n subcarriers, the first "S_n" available subcarriers of the base station have to be simultaneously scanned. This leads to a complexity of $\boldsymbol{O}(S_n)$.

In the case of the *FFR* (where 2 concentric sub-regions per cell are considered), if $C=|C_b|$, then the complexity is calculated equal to $\boldsymbol{O}[(C/2)* S_n]$.

In the case of the *anti-EMI* strategy, if J_{bs} is the number of neighbouring *BS*s which serve the *Jammers*, then the subcarrier frequencies C (where $C=|C_b|$) of the J_{bs} neighbouring base stations and the b^{th} BS must be scanned. This scan leads to a preliminary complexity equal to $\boldsymbol{O}[(J_{bs}+1)*C]$. Since the procedure repeats for S_n number of subcarrier frequencies, the complexity finally equals $\boldsymbol{O}[(J_{bs}+1)*C* S_n]$.

The algorithmic complexity of *GRID* equals $\boldsymbol{O}[[length(f)*(J+1)+C]* S_n]$, where J is the maximum number of *Jamming edge sub-blocks* ($J = \sqrt{G}+1$). Therefore, (in the worst case scenario) the subcarrier subsets J of the neighbouring base stations and the serving BS must be scanned, which leads to a preliminary complexity $\boldsymbol{O}[length(f)*(J+1)]$. If in this case there are no available subcarriers, all subcarriers C_b (where $C=|C_b|$) of the BS must be scanned resulting in $\boldsymbol{O}[length(f)*(J+1)+C]$. Since the procedure repeats for all the S_n number of subcarrier frequencies the algorithmic complexity finally equals $\boldsymbol{O}[[length(f)*(J+1)+ C]* S_n]$.

VI. SIMULATIONS

In all simulation scenarios, we have considered 30% and 50% *PF* (probability failure), 1 and 2 tiers of BSs and 156.25 Kbps, 312.5 Kbps and 39.625 Kbps per MT (QPSK modulation [42]). It is noted that we have considered high values of PF instead of lower, i.e. 5%, only for evaluation purposes. In order to compare the strategies and evaluate them on a common basis, fixed number of subcarriers per MT is considered. As such, not only the capacity-power problem is relatively simplified, but also the MTs are permitted to judiciously have access to the radio resources. In case $S_n \geq |C_b|$, the b^{th} BS cannot establish new links and *hard blocking* occurs (new connections are blocked). Moreover, to obtain representative mean values of the mean capacity, mean total power dissipation (the power dissipated at the circuits of the transceiver and other parts is not included), etc., the platform executes a sufficient number of MC snapshots. In our case, to establish upper bounds for the number of MC runs, elementary Case-Based Reasoning (CBR) [43] is used. It has been noticed all investigated metrics were converging to their mean value after 10^3 MC runs approximately.

The performance of all the subcarrier allocation strategies (namely *Round Robin, FFR, GRID, anti-EMI*) is presented in Fig. 8-9. The *FFR* is studied for 2 sub-regions per cell, the *anti-EMI* is evaluated for two *JR* values (1 *Km*, 1.5 *Km*), while *GRID* is evaluated for 4, 9, 16, 25 and 36 sub-blocks per block/BS. Overall, for all strategies, the mean throughput and the mean total power dissipated by the whole system decrease as the number of subcarrier frequencies increases. This makes sense because when the MTs are assigned a high number of subcarriers, then the likelihood to jam each other and leave the network is higher; hence throughputs decrease and less power is dissipated.

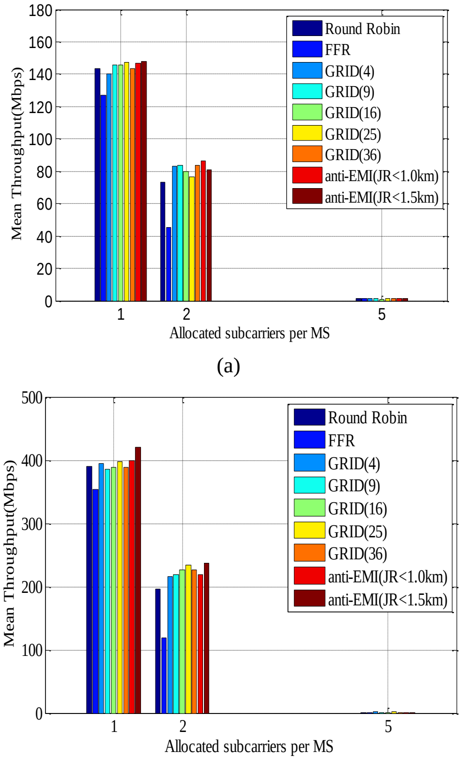

(a)

(b)

Fig. 8. Mean Throughput (Kbps) for PF = 30%, (a) 1 tier and (b) 2 tiers.

In detail, *anti-EMI(JR<1 Km)* performs better than *anti-EMI (JR<1.5 Km)* {8% mean throughput gain for 30%, 2 tiers and 2 subcarriers per MT}. From this, it can be concluded that the strength of the signal of the *Jammers* which are located 1 *Km* away from the n^{th} MT is not so intense; hence it does not really matter whether the n^{th} MT shares with them common radio resources or not. In the just-mentioned scenario, *anti-EMI (JR<1 Km)* and *GRID(25)* behave the same (9 bps difference). As for the *GRID* algorithm, *GRID(25)* outperforms all the other configurations, with *GRID(16)* being the worst.

In general, *GRID* competes *anti-EMI* in the majority of the scenarios into consideration, while *Round Robin* is the worst of all algorithms. This happens because *Round Robin* assigns to the terminals adjacent subcarriers which experience correlated fading; hence it is very likely that the quality of all allocated subcarriers of a terminal is low. *Round Robin* performs well (ranks third) in two scenarios: {*PF*, Tiers, Subcarriers/MT} = {50%, 1, 5} and {*PF*, Tiers, Subcarriers/MT} = {50%, 2, 1}. In quite all scenarios, *anti-EMI(JR<1 Km)* competes *GRID(25)*. It is also noted that *Round Robin* outperforms neither *GRID* nor *anti-EMI*.

Moreover Fig. 9 reveals that for 1 subcarrier, all strategies allow the 80% approximately of the maximum Throughput to be supported and for 2 subcarriers the 50%. In Fig. 9, for 1 subcarrier less than 90% of the maximum Throughput is supported, for 2 subcarriers less than 70%, while for 5 subcarriers 10%.

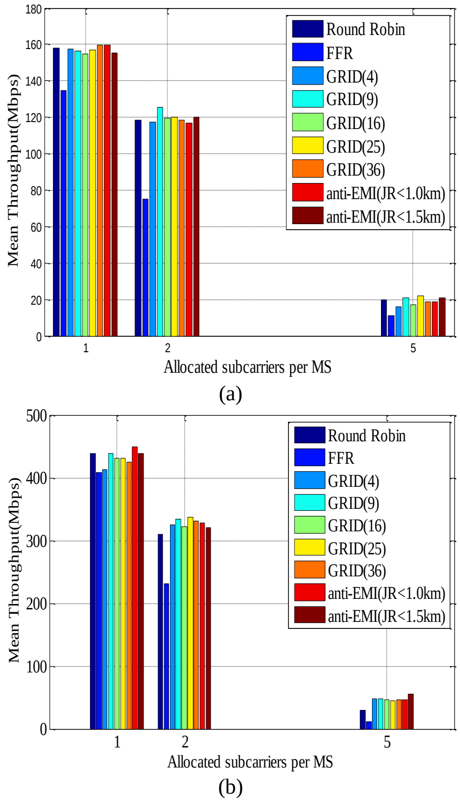

(a)

(b)

Fig. 9. Mean Throughput (Kbps) for PF = 50%, (a) 1 tier and (b) 2 tiers.

Fig. 10 provides the total dissipated power only for PF = 30 %. If scaled up, these results are representative and apply for PF = 50 % scenarios as well. To better understand what is depicted, suppose that a MT consumes the maximum available power, that is to say 1 Watt (worst case, Eq. 3b). For 140 Mbps approx. (1 subcarrier per MT, Fig. 10), 896 MTs are served in total by the network. Therefore, in the worst case, the power profile of the overall system would equal 896 Watts (maximum). However, simulations show that the power in this specific case is equal to 210 approx. no matter what strategy is implemented. When 2 subcarriers per MT are considered in a 1-tier scenario, 256 MTs are served and consume 80 Watts (instead of 256 Watts). As a result, it is straightforward that the gains in power reach the 76% and 68% respectively. For 2 tiers and 1 (400 Mbps or 2560 MTs) and 2 (210 Mbps or 672 MTs) subcarriers per MT, the power profile of the network is 600 Watts (instead of 2560 Watts) and 220 Watts (instead of 672 Watts) respectively. As a result, it is straightforward that the gains in power reach the 76% and 67% respectively. Due to the fact that 5 subcarriers per MT lead to very low mean throughputs and subsequently to a very low total power dissipation, we cannot extract much information for the power efficiency that the platform is capable to provide; hence we let aside such scenarios. However, we comment on highly populated scenarios as in the case of 1 and 2 subcarriers per MT. Overall, Fig. 10 shows the platform can spare around the 70% of the maximum available power.

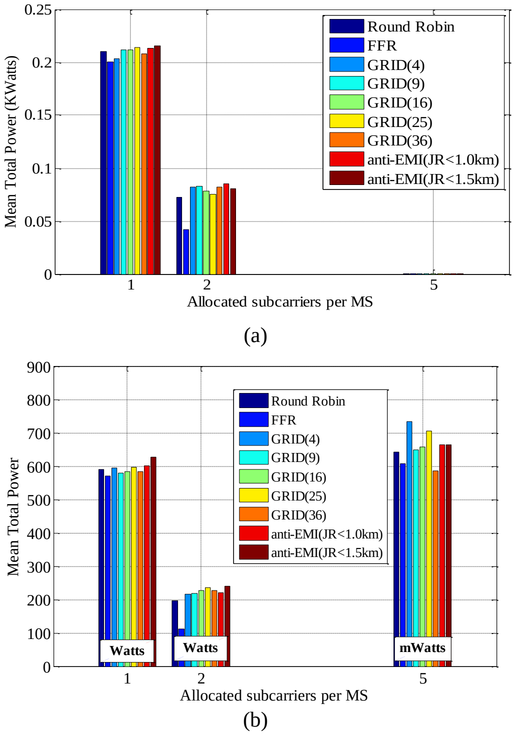

(a)

(b)

Fig. 10. Mean Total Power (KWatts) for PF = 30%, SINR = 9.6dB, 1 tier.

VII. CONCLUSIONS

In this paper, the performance of two resource allocation strategies (*GRID*, *anti-EMI*) for large OFDMA networks with cell of arbitrary shapes is analyzed and evaluated after comparison with the *Round Robin* and the traditional *FFR*. Prior to any MC simulation, the *GRID* conceptually grids the spatial area around each BS into blocks. Each block is likewise partitioned in sub-blocks, which are allocated a disjoint subset of subcarrier frequencies. Once a mobile terminal gains access to the network, it is assigned radio resources which correspond to its geographical sub-block. The strategy outperforms the *Round Robin* and the traditional *FFR* algorithms and competes the *anti-EMI* strategy especially when 25 sub-blocks per BS are considered, thanks to the spatial isolation which offers to the mobile terminals. As for the *anti-EMI*, the strategy classifies the terminals of the neighboring BSs into *Jammers* and *non-Jammers* according to a predefined distance from each last accepted MT and, then, provides the terminal with the subcarriers which are not reused by the *Jammers*. In other words, *anti-EMI* partitions the area around each MT, which has been accepted last. Overall, the *GRID* and the *anti-EMI* strategies judiciously increase the mean throughput by mitigating CCI; hence spectral efficiency is enhanced, and do not load the system with extra overhead (resource allocation without CSI). Additionally, the *GRID* strategy does not increase further the computational overhead (physical space is gridded prior to MC snapshots). Finally, the platform can inherently spare around the 70% of the maximum available power.

ACKNOWLEDGEMENTS

This research has been co-financed by the European Union (European Social Fund - ESF) and Greek national funds through the Operational Program “Education and Lifelong Learning” of the National Strategic Reference Framework (NSRF)-Research Funding Program: THALIS – NTUA, “Novel Transmit and Design Techniques for Broadband Wireless Networks” (MIS 379489).

REFERENCES

[1] URL: https://www.itu.int/en/ITU-D/Statistics/Pages/stat/default.aspx

[2] A. Goldsmith, “Wireless Communications”, Stanford University, 2005.

[3] IEEE, IEEE standard for local and metropolitan area networks, Part 16, IEEE 802.16-2004, New York, NY, 2004.

[4] "IEEE Std 802.15.1–2005 – IEEE Standard for Information technology – Telecommunications and information exchange between systems – Local and metropolitan area networks – Specific requirements Part 15.1: Wireless Medium Access Control (MAC) and Physical Layer (PHY) Specifications for Wireless Personal Area Networks (W Pans)", 2010.

[5] ANSI/IEEE Std 802.11, Wireless Lan medium access control (MAC) and physical layer (PHY) specifications, 1999.

[6] "IEEE 802 LAN/MAN Standards Committee 802.22 WG on WRANs (Wireless Regional Area Networks)", 2009.

[7] G. Li and H. Liu, “Downlink Radio Resource Allocation for Multi-Cell OFDMA System,” IEEE Transactions on Wireless Communications, vol. 5, no. 12, pp. 3451-3459, 2006.

[8] H. Kwon, H. Seo and S. Kim, "Generalized CSMA/CA for OFDMA Systems: Protocol Design, Throughput Analysis, and Implementation Issues", IEEE Transactions on Wireless Communications, vol. 8, no. 8, pp. 4176-4187, August 2009.

[9] H. Kwon, S. Kim and B. G. Lee, "Opportunistic multi-channel CSMA protocol for OFDMA systems", IEEE Trans. Wireless Commun., vol. 9, no. 5, pp. 1552-1557, 2010.

[10] S.G.Yoon, D. Kang et al., "Multichannel CSMA/CA protocol for OFDMA-based broadband power-line communications", IEEE Trans. Power Del., vol. 28, no. 4, pp. 2491-2499, Oct. 2013.

[11] G. Haile and Jaesung Lim, "C-OFDMA: Improved Throughput for Next Generation WLAN Systems Based on OFDMA and CSMA/CA", 4th International Conference on Intelligent Systems Modelling Simulation (ISMS), pp. 497-502, January 2013.

[12] Q. Qu, B. Li, M. Yang and Z. Yan, "An OFDMA based concurrent multiuser MAC for upcoming IEEE 802.11ax", Wireless Communications and Networking Conference Workshops (WCNCW), pp. 136 - 141, March 2015.

[13] H. Zhou, B. Li, Zh. Yan, M. Yang and Q. Qu, "An OFDMA based multiple access protocol with QoS guarantee for next generation WLAN", IEEE International Conference on Signal Processing, Communications and Computing (ICSPCC), pp. 1 - 6, September 2015.

[14] Y. P. Fallah, S. Khan, P. Nasiopoulos and H. M. Alnuweiri, "Hybrid OFDMA/CSMA based medium access control for next-generation wireless LANs", IEEE International Conference on Communications, pp. 2762-2768, May 2008.

[15] T. Jiang, L. Song, and Y. Zhang, Orthogonal Frequency Division Multiple Access Fundamentals and Applications, Boston MA, USA: Auerbach Publications, 2010.

[16] Li J., Botella C. and Svensson T., “Resource allocation for clustered network MIMO-OFDMA systems”. EURASIP Journal on Wireless Communications and Networking 2012: 175, DOI: 10.1186/1687/1499/2012/175.

[17] Chang R. Y., Tao Z. F., Zhang J. Y. and Kuo C-C. J., “Dynamic fractional frequency reuse (D/FFR) for multicell OFDMA networks using a graph framework”. Wireless Communications and Mobile Computing 2013, vol. 13, no. 1, 2013.

[18] Choi B., Lim S. and Lee T. J., “Sequential frequency reuse with power control for OFDMA systems”. Wireless Communications and Mobile Computing 2013; vol. 13, no. 1, 2013.

[19] D. Bilios, C. Bouras, V. Kokkinos, A. Papazois, G. Tseliou, A performance study of fractional frequency reuse in OFDMA networks, in: Wireless and Mobile Networking Conf. (WMNC), Paris, France, pp. 38–43, 2012

[20] M. Amer, Optimal configuration of fractional frequency reuse system for LTE cellular networks, IEEE Veh. Technol. Conf. (VTC), Québec City, Canada, pp. 1–5, 2012.

[21] M. Qian, W. Hardjawana, Y. Li, B. Vucetic, X. Yang, and J. Shi,“Adaptive soft frequency reuse scheme for wireless cellular networks,” on Vehicular Technology, IEEE Transactions, vol. 64, no. 1, pp. 188–131, 2014.

[22] D. Gonzalez, M. Garcia-Lozano, S. Ruiz and J. Olmos, “On the Performance of Static Inter-cell Interference Coordination in Realistic Cellular Layouts,” Mobile Networks and Management (MONAMI 2010), Lecture Notes of the Institute for Computer Sciences, Social Informatics and Telecommunications Engineering (LNICST), vol. 68, no. 4, pp.163-176, 2011.

[23] D. Gonzalez, M. Garcia-Lozano, S. Ruiz, and J. Olmos, “On the Need for Dynamic Downlink Intercell Interference Coordination for Realistic LTE Deployments,” Wireless Communications and Mobile Computing, vol. 14, no. 4, pp. 409-434, March 2014.

[24] L. Chen and D. Yuan, “Soft frequency reuse in large networks with irregular cell pattern: How much gain to expect?,” in Proc. IEEE 20th Int Personal, Indoor and Mobile Radio Communications Symp., pp. 1467-1471, 2009.

[25] European project IST-2000-28088. URL: http://momentum.zib.de, 2005.

[26] D. Gonzalez, M. Garcia-Lozano, S. Ruiz and M. Lema, "Adapting fractional frequency reuse to realistic OFDMA cellular networks," 6th Joint IFIP Wireless and Mobile Networking Conference (WMNC), Dubai, pp. 1-8, April 2013.

[27] L. Chen and D. Yuan, "Generalized frequency reuse schemes for OFDMA networks: optimization and comparison", Proc. 2008 IEEE VTC - Fall, pp. 1-5, 2008.

[28] C. A. Coello, G. B. Lamont, and D. A. Van Veldhuizen, Evolutionary Algorithms for Solving Multi-Objective Problems, 2nd ed. Springer: Genetic and Evolutionary Computation Series, 2007.

[29] K. Deb, A. Pratap, S. Agarwal, and T. Meyarivan, “A Fast and Elitist Multiobjective Genetic Algorithm: NSGA-II,” on Evolutionary Computation, IEEE Transactions, vol. 6, no. 2, Apr 2002.

[30] C. Lei and D. Yuan, “Generalizing and Optimizing Fractional Frequency Reuse in Broadband Cellular Radio Access Networks,” EURASIP Journal on Wireless Communications and Networking 2012, vol. 2012, pp. 1-15, 2012.

[31] R. Ullah, N. Fisal, H. Safdar, W. Maqbool, Z. Khalid and A. S. Khan, "Performance Enhancement of LTE through Interference Reduction Techniques," Universal Journal of Communications and Network, vol. 2, no. 3, pp. 58-62, 2014.

[32] O. Aliu, M. Mehta, M. Imran, A. Karandikar and B. Evans, "A new cellular-automata-based fractional frequency reuse scheme", IEEE Trans. Veh. Technol., vol. 64, no. 4, pp. 1535-1547, 2015.

[33] Andrews, R. Ganti, M. Haenggi, N. Jindal, and S. Weber, "A primer on spatial modelling and analysis in wireless networks," Communications Magazine, IEEE, vol. 48, no. 11, pp. 156-163, 2010.

[34] R. Ullah, N. Fisal, H. Safdar, W. Maqbool, Z. Khalid and A. Khan, "Voronoi cell geometry based dynamic fractional frequency reuse for ofdma cellular networks", IEEE International Conference on Signal and Image Processing Applications (ICSIPA) 2013, pp. 435-440, 2013.

[35] J. Xu, J. Zhang, and J. Andrews, "On the accuracy of the wyner model in cellular networks," on Wireless Communications, IEEE Transactions, vol. 10, no. 9, pp. 3098-3109, 2011.

[36] M. Haenggi, J. Andrews, F. Baccelli, O. Dousse, and M. Franceschetti, "Stochastic geometry and random graphs for the analysis and design of wireless networks," on Selected Areas in Communications, IEEE Journal, vol. 27, no. 7, pp. 1029-1046,2009.

[37] Andrews, "Seven ways that hetnets are a cellular paradigm shift,"Communications Magazine, IEEE, vol. 51, no. 3, pp. 136-144, 2013.

[38] L. Chen and D. Yuan, “Generalizing FFR by Flexible Sub-Band Allocation in OFDMA Networks with Irregular Cell Layout,” in Wireless Communications and Networking Conference Workshops (WCNCW), 2010 IEEE, pp. 1–5, April 2010.

[39] Evolved universal terrestrial radio access network (E-UTRAN); X2 application protocol (X2AP) (Rel. 9), 3rd Generation Partnership Project, Cedex, France, 3GPP Tech. Spec. TS 36.423 V9.5.0.

[40] 3GPP TR 25.996 v6.1.0, “Spatial Channel model for Multiple Input Multiple Output (MIMO) simulations”, September 2003.

[41] J.G. Andrews, A. Ghosh, R. Muhamed, Fundamentals of WiMAX: understanding broadband wireless networking, First ed., Prentice Hall, PTR, Upper Saddle River, NJ, 2007.

[42] Giuliano R., Monti C. WiMax Fractional Frequency Reuse for Rural Environments, IEEE Wireless Communications 2008; vol. 1, no. 3, pp. 60-65, 2008.

[43] A. Aamodt, and E. Plaza, Case-Based Reasoning: Foundational Issues, Methodological Variations, and System Approaches, Artificial Intelligence Communications, vol. 7, no. 1, pp. 39-52, 1994.

Maria A. Seimeni received her Diploma from the ECE School of Democritus University of Thrace (DUTh), her MSc at Politecnico di Torino (PoliTo) and her PhD from the ECE School of National Technical University of Athens (NTUA) in 2007, 2009 and 2016 respectively. In 2017, she joined the R&D department of Singular Logic SA, where she acts as a researcher covering projects' administration and implementation and the bidding of National/European calls mainly focusing on ESA ITTs. She collaborates with the ICBNet and MFOL Laboratories (NTUA) since 2012, the department of Electrical Engineering, Mathematics & Computer Science of the University of Twente (UT, NL) in the frame of COST Action IC1407 and the National Observatory of Athens/Uni.of Peloponnese in the frame of a Space MSc Program as a member of their Teaching Staff. Till 2016, she was involved with ESA in few contracts (Tests Engineer, Tests Manager/Supervisor, EMC Project Manager), whereas till 2009 she was working for Leonardo Aerospace, Defence and Security (formerly Alenia Aeronautica S.p.A.) as EMC Tests Engineer. Her scientific interests are in the field of Wireless OFDMA/MIMO systems, EMC, Wearable Antennae and Microwave Circuits Design. She is a reviewer in International Scientific Journals with impact and peer-reviewed International Scientific Conferences.

Georgios I. Tsivgoulis received the Bachelor degree in marine engineering from the Hellenic Naval Academy (HNA) in 2001 and the MSc in electrical engineering and the electrical engineer Degree from the U.S Naval Postgraduate School (NPS) in 2009. He is currently working towards his PhD in telecommunications in ICBNet of the National Technical University of Athens (NTUA). Georgios Tsivgoulis served as electrical and electronics engineer and as chief engineer onboard various warships of the Hellenic Navy and as deputy technical manager in the Hellenic Navy’s Frigate Command. In 2015, he joined Thenamaris Ships Management Inc., Athens, where he is holding the position of the Electrical Supervisor leading a team of electrical engineers responsible for the electronics, radio navigation, telecommunications, electrical and automation systems of the managed vessels. His research interests include: transmission techniques in multi-cellular MIMO/OFDMA systems, VSAT communications, wireless sensor networks and digital signal processing. Georgios Tsivgoulis is a Registered Electrical Engineer and member of the Technical Chamber of Greece.

Panagiotis K. Gkonis was born in Athens, Greece in 30 August 1981. He received his Diploma Degree in Electrical and Computer Engineering and PhD degree from the Electrical and Computer Engineering School of the National Technical University of Athens (NTUA), Greece, in 2005 and 2009, respectively. He currently works as a postdoctoral researcher in the Intelligent Communication and Broadband Networks Laboratory (ICBNet) of NTUA. He is also a member of the Technical Chamber of Greece.

Dimitra I. Kaklamani was born in Athens, Greece, in 1965. She received the PhD degree from the National Technical University of Athens (NTUA) in electrical and computer engineering (ECE), in 1992. In April 1995, April 2000, October 2004, and February 2009, she was elected Lecturer, Assistant Professor, Associate Professor, and Professor, respectively, with the School of ECE, NTUA. She has more than 260 publications in the fields of software development for information transmission systems modelling, microwave networks, mobile and satellite communications, and has coordinated the NTUA activities in the framework of several EU and National projects in the same areas. She is Editor of one international book by Springer-Verlag (2000) in applied CEM and reviewer for several IEEE journals.

Iakovos S. Venieris is a Professor in the School of Electrical and Computer Engineering, National Technical University of Athens (NTUA) since 1994 and director of ICBNet. He received the Dipl.-Ing. degree from the University of Patras, Patras, Greece in 1988, and the Ph.D. degree from the NTUA in 1990, all in Electrical and Computer Engineering. His research interests are in the fields of distributed systems, security and privacy, software and service engineering, agent technology, multimedia, mobile communications and intelligent networks, internetworking, signalling, resource scheduling and allocation for network management, modelling, performance evaluation, queuing theory. He has over 350 publications in the above areas and has received several national and international awards for academic achievement. He has participated in and has successfully led several national and international projects. He is a reviewer for several IEEE, ACM, Elsevier and Wiley journals and has served as associate editor of IEEE Communications Letters, editorial board member of Computer Communications (Elsevier) and guest editor for the IEEE Communications Magazine. He is a co-editor of the books Intelligent Broadband Networks (Wiley, 1998) and Object Oriented Software Technologies in Telecommunications (Wiley, 2000).

Christos A. Papavassiliou (M’96–SM’05) was born in Athens, Greece, in 1960. He received the B.Sc. degree in physics from the Massachusetts Institute of Technology, and the Ph.D. degree in applied physics from Yale University. He has worked on GaAs monolithic microwave integrated circuit (MMIC) design and measurements with Foundation for Research and Technology, Hellas, Crete, Greece, and was involved in several European and regional projects on GaAs MMIC technology. Since 1996 he has been at Imperial College London, where he has worked on SiGe technology development, RF IC, and instrumentation. He has contributed to over 70 publications. His current research interests include memristor applications, surface wave propagation on interfaces and antenna arrays.